



Deformation of Mexico from continuous GPS from 1993 to 2008

B. Marquez-Azua

DGOT, SisVoc, Universidad de Guadalajara, Avenida Maestros y Mariano Barcenas, 93106, Guadalajara, Jalisco, Mexico

C. DeMets

Department of Geology and Geophysics, University of Wisconsin-Madison, 1215 Dayton, Madison, Wisconsin 53706, USA (chuck@geology.wisc.edu)

[1] We combine the velocities of 13 continuous Global Positioning System stations from Mexico and 448 North American plate stations to better understand deformation and earthquake cycle effects in Mexico. Velocities estimated at the Mexican sites from high-quality GPS data collected since 2003 show no evidence for a previously reported eastward bias at sites in and near the Yucatan peninsula. The new velocities are compared to the predictions of two models, one in which all motion in Mexico is attributed to North American plate motion and the second of which attributes site motions to a combination of plate motion and the elastic effects of frictional coupling along the Mexican subduction zone and faults in the Gulf of California. The second model fits the velocities within their estimated uncertainties. Mainland Mexico thus moves with the North American plate to within 1 mm per year and undergoes elastic interseismic deformation far into its interior. Two stations inland from the Guerrero and Oaxaca segments of the Mexican subduction zone have alternated between several-year-long periods of landward motion and several-month-long periods of trenchward motion frequently since 1993, consistent with previously described, repeating transient slip events along the subduction interface. The motions of two stations inland from the Rivera plate subduction zone are dominated by the coseismic and postseismic effects of the $M = 8.0$, 9 October 1995 Colima-Jalisco earthquake and $M = 7.5$, 22 January 2003 Tecoman earthquake offshore from western Mexico.

Components: 8529 words, 8 figures, 2 tables.

Keywords: tectonics.

Index Terms: 1240 Geodesy and Gravity: Satellite geodesy: results (6929, 7215, 7230, 7240); 1207 Geodesy and Gravity: Transient deformation (6924, 7230, 7240); 1209 Geodesy and Gravity: Tectonic deformation (6924).

Received 11 October 2008; **Revised** 2 December 2008; **Accepted** 22 December 2008; **Published** 6 February 2009.

Marquez-Azua, B., and C. DeMets (2009), Deformation of Mexico from continuous GPS from 1993 to 2008, *Geochem. Geophys. Geosyst.*, 10, Q02003, doi:10.1029/2008GC002278.

1. Introduction

[2] Over the past decade, continuous and campaign Global Positioning System (GPS) measurements in

Mexico have established an increasingly reliable basis for addressing questions about deformation within this tectonically active country. To date, most GPS studies in Mexico have focused on

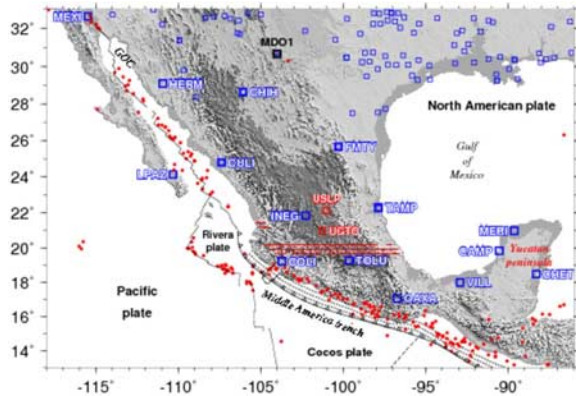


Figure 1. Tectonic setting, seismicity, topography, and location map for the study area. Red circles show epicenters of all 1963–2008 earthquakes with magnitudes greater than 5.5 and depths above 40 km and are from the U.S. Geological Survey National Earthquake Information Center files. Labeled blue squares specify locations and names of the 15 continuous RGNA GPS stations that are the subject of this study. Smaller blue squares indicate the locations of other continuous GPS stations whose motions are used herein. Red squares and labels indicate recently installed RGNA sites not used for this analysis. Area indicated by horizontal red stripes is the Mexican volcanic belt. Open circles between trench and coast are surface-projected node locations that approximate locked areas of the subduction interface for elastic calculations described in text. “GOC” is Gulf of California.

regions located between the Pacific coast and Mexican volcanic belt (Figure 1), where large-magnitude earthquakes along the Mexican subduction zone pose a significant hazard. Such studies have revealed significantly more complex earthquake cycle deformation than was imagined less than a decade ago. In particular, GPS measurements clearly establish that frequent transient, aseismic slip occurs along the Guerrero and Oaxaca segments of the subduction interface, raising important questions about whether such slip influences the timing of large subduction zone earthquakes [Lowry *et al.*, 2001; Kostoglodov *et al.*, 2003; Yoshioka *et al.*, 2004; Franco *et al.*, 2005; Brudzinski *et al.*, 2007; Larson *et al.*, 2007; Correa-Mora *et al.*, 2008; F. Correa-Mora *et al.*, Transient deformation in southern Mexico in 2006 and 2007: Evidence for distinct deep-slip patches beneath Guerrero and Oaxaca, submitted to *Geochemistry, Geophysics, Geosystems*, 2009].

[3] Complementing this work, questions about the large-scale tectonics of Mexico are addressed by

Marquez-Azua and DeMets [2003] and Marquez-Azua *et al.* [2004] using continuous GPS measurements from a 15-station nationwide GPS network that has been operated by the Mexican government since 1993 (Figure 1). On the basis of non-P-code GPS data that were collected prior to mid-2001, Marquez-Azua and DeMets [2003, hereinafter referred to as MD2003] conclude that GPS stations north of the Mexican Volcanic Belt move with the North America plate within their $1\text{--}2\text{ mm a}^{-1}$ velocity uncertainties but that stations south of the volcanic belt, most notably in the Yucatan peninsula, move $1\text{--}4\text{ mm a}^{-1}$ to the east relative to the North American plate. MD2003 examine whether this unexpected eastward motion could be an artifact of the non-P-code GPS data that were used to determine the station velocities or whether any geologic evidence supports the slow eastward movement of southern Mexico but find no compelling evidence for either explanation.

[4] In this study, we use an additional 7 years of continuous measurements from 13 of the 15 GPS stations that were used by MD2003 to revisit questions about the large-scale tectonics of mainland Mexico. New data from the other two stations used by MD2003, namely, LPAZ and MEXI in Baja and Alta California, provide little information relevant to this study and are not reported here since the station velocities have not changed substantially. Critically, the new GPS data include high-quality P-code and carrier phase data that have been recorded continuously since early 2003. These data provide an independent test of the accuracy of the MD2003 station velocities and are used below to estimate a useful new upper bound on possible motion across the Mexican volcanic belt. The motions of four RGNA stations that record coseismic, postseismic, interseismic, and transient-slip processes caused by subduction of the Rivera and Cocos plates constitute the longest continuous records of earthquake cycle deformation in Mexico and are presented and described here for the first time for the benefit of future investigators.

2. Tectonic Setting

[5] The active deformation of Mexico is caused primarily by the interactions between five tectonic plates that share boundaries within or near Mexico (Figure 1). Along the Mexican segment of the Middle America trench (Figure 1), the Rivera and Cocos plates subduct at rates that increase from



Table 1. RGNA Site Velocities in ITRF2005^a

Site	Latitude °N	Longitude °W	Velocities		Correlation Coefficient
			$V_n \pm 1\sigma$	$V_e \pm 1\sigma$	
CAMP	19.845	90.540	-0.5 ± 0.5	-8.1 ± 0.5	0.029
CHET	18.495	88.299	0.4 ± 0.5	-7.4 ± 0.6	-0.166
CHIH	28.662	106.087	-6.6 ± 0.5	-11.4 ± 0.6	-0.045
COLI	19.244	103.702	–	–	–
CULI	24.799	107.384	-6.9 ± 0.5	-9.3 ± 1.1	-0.156
FMTY	25.715	100.313	-4.8 ± 0.6	-10.3 ± 0.6	-0.043
HERM	29.093	110.967	-7.2 ± 0.5	-12.1 ± 0.6	-0.044
INEG	21.856	102.284	-4.9 ± 0.5	-8.4 ± 0.7	0.060
MERI	20.980	89.620	-0.1 ± 0.5	-8.5 ± 0.5	-0.022
OAXA	17.078	96.717	0.8 ± 0.9	-2.9 ± 0.9	0.373
TAMP	22.278	97.864	-4.5 ± 0.5	-9.0 ± 0.7	0.111
TOLU	19.293	99.644	-2.0 ± 0.8	-5.3 ± 0.6	-0.008
VILL	17.990	92.931	0.8 ± 0.5	-8.2 ± 0.6	-0.122

^aRGNA station locations and horizontal velocities. Best-fitting velocities are determined for the period 20 January 2003 to 1 August 2008. No velocity is given for site COLI, whose motion is dominated by the postseismic effects of the 22 January 2003 Tecoman earthquake. North and east velocity components are specified by V_n and V_e , respectively, and are in units of millimeters per year. Geodetic latitudes are specified.

$\sim 20 \text{ mm a}^{-1}$ at the northwestern end of the trench [DeMets and Wilson, 1997] to $\sim 80 \text{ mm a}^{-1}$ near the Mexico-Guatemala border [DeMets, 2001]. The elastic effects associated with this subduction have been measured hundreds of kilometers inland from the Pacific coast [Yoshioka et al., 2004; Correa-Mora et al., 2008] and dominate interseismic deformation in southern and western Mexico. In the Gulf of California (Figure 1), motion between the Pacific and North American plates is partitioned between faults in the gulf, which accommodate $\sim 48 \text{ mm a}^{-1}$ of dextral strike-slip motion [DeMets, 1995], and faults within and west of the Baja California peninsula [Michaud et al., 2004], which accommodate an additional 3 to 5 mm a^{-1} of dextral slip [Dixon et al., 2000; Plattner et al., 2007]. In the state of Chiapas in southern Mexico, distributed faulting and folding occurs in response to motion between the Caribbean and North American plates [Guzman-Speziale et al., 1989; Guzman-Speziale and Meneses-Rocha, 2000].

[6] The other major tectonic feature in Mexico is the Mexican Volcanic Belt, which extends $\sim 900 \text{ km}$ across central Mexico (Figure 1) and poses significant volcanic and seismic hazards to interior areas of the country. Recent structural studies of faults that displace Quaternary-age rocks in the central part of the volcanic belt suggest that the bulk Neogene motion across the volcanic belt has been limited to NNW–SSE-oriented extension of $0.2 \pm 0.05 \text{ mm a}^{-1}$ [Suter et al., 2001; Langridge et al., 2000]. Similarly, the estimated Quaternary deformation rate across faults at the western end of the

volcanic belt is only 0.1 mm a^{-1} [Ferrari and Rosas-Elguera, 2000].

3. Data

[7] The primary data emphasized in this analysis are from the Red Geodesica Nacional Activa (RGNA), a continuous GPS network operated by the Mexican government agency Institutos Nacionales Estadística y Geografía (INEGI). The RGNA network presently consists of 17 continuous GPS stations (Figure 1), of which 15 have operated continuously for more than a decade and are used for this analysis (Table 1) and two were added after 2007 (UGTO and USLP). Since mid-2004, all RGNA data have been openly available for a 90-day window after the data are collected. Access to the proprietary data from times before 2004 has been granted to the University of Guadalajara via a negotiated legal agreement. Logistical factors limited our access to data collected before mid-2001 to one station-day per week [Marquez-Azua and DeMets, 2003]. Daily data are used for times after mid-2001.

[8] Operation of the RGNA network commenced at 14 stations during February to April of 1993 and at a 15th station (CAMP) in September of 1995. All 15 stations were originally equipped with Ashtech LM-XII3 receivers and antennas, which acquire coarse-acquisition (C/A) code and L1 and L2 phase information but do not collect P-code observables under antispoofing conditions. In February of 2000, the equipment at station INEG

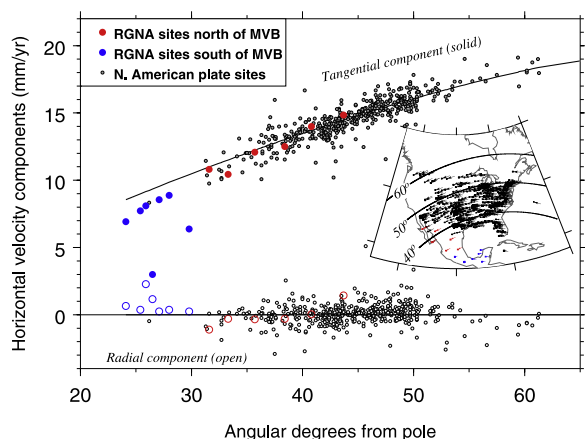


Figure 2. Components of North American plate GPS velocities that are locally parallel (tangential) and orthogonal (radial) to small circles centered on the angular velocity vector that best describes North American plate motion relative to ITRF05. Inset shows the locations of stations used to determine the best-fitting angular velocity vector given in Table 2. The small circles labeled 40°, 50°, and 60° in the inset indicate angular distances from the best-fitting pole and are the same as on the horizontal axis of the upper panel. Blue and red symbols indicate RGNA stations located south and north of the Mexican Volcanic Belt, respectively. Uncertainties are omitted for clarity but are typically $\pm 1 \text{ mm a}^{-1}$ or smaller.

was upgraded to a dual-frequency, P-code Trimble receiver and choke ring antenna. Upgrades to dual-frequency, P-code Trimble receivers with Zephyr geodetic antennas occurred at 13 additional stations in January of 2003 and at the remaining station (FMTY) in September of 2003. Readers are referred to MD2003 and www.inegi.org.mx/inegi for additional information about the RGNA network.

[9] Physical relocations of the GPS antennas have occurred at least once since 1993 at nine of the 15 RGNA stations. Only one of these antenna relocations merits discussion, namely, the relocation in August of 2001 of the antenna at station TOLU to a location 625 m away. Prior to this antenna relocation, the station moved erratically, including 50 mm of subsidence in the 3 years prior to the antenna relocation. No further vertical movement has occurred since the antenna was relocated and the horizontal components of the station motion are also well behaved. It thus seems likely that instability of the building or monument that hosted the antenna prior to its relocation was the source of the erratic station behavior, rather than volcanic

deformation or localized subsidence due to groundwater withdrawal, as were postulated by MD2003.

[10] Precise geodetic ties between the old and new RGNA antenna locations are not available for any of the stations. We therefore estimate all antenna offsets as part of our postprocessing of the station coordinate time series. All of the Ashtech antennas exhibit sudden 25–50 mm westward offsets in their estimated phase center longitudes in mid-August of 1999 even though none of the antennas was physically relocated then [Marquez-Azua and DeMets, 2003]. These offsets coincided with the installation of new Ashtech receiver firmware that was designed to handle the GPS week roll-over that occurred at that time. Given that other types of GPS receivers did not exhibit similar shifts in their antenna phase centers during the GPS week roll-over in 1999, it seems likely that the Ashtech LM-XII3 receiver firmware prior to August of 1999 corrupted one or both of the phase or code measurements that were collected prior to this time. Further evidence for a bias in the eastward components of the estimated station motions before 1999 is given below.

[11] We also use continuous GPS data from 448 sites outside of Mexico (Figure 2) to estimate an angular velocity vector for the North American plate relative to ITRF05. All 448 stations have operated continuously for 3 years or longer and are located outside deforming areas of the western United States and Canada [Bennett *et al.*, 1999] and outside areas of significant postglacial rebound in Canada and the north central and northeastern United States [Calais *et al.*, 2006; Sella *et al.*, 2007].

4. Methods

4.1. GPS Station Velocities and Uncertainties

[12] We processed all of the GPS data described above with GIPSY software (release 4) from the Jet Propulsion Laboratory (JPL). We apply a precise point-positioning analysis strategy [Zumberge *et al.*, 1997] and use fiducial-free satellite orbits and satellite clock corrections from JPL. Daily station locations are estimated initially in a no-fiducial reference frame [Heflin *et al.*, 1992] and are transformed to ITRF2005 [Altamimi *et al.*, 2007] using daily seven-parameter Helmert transformations from JPL. Postprocessing procedures are also applied to estimate and remove spatially correlated

Table 2. Best-Fitting North American Plate Angular Velocity Vector^a

Plate	N	χ^2_ν	Angular Velocity			Covariances					
			Latitude	Longitude	ω	σ_{xx}	σ_{yy}	σ_{zz}	σ_{xy}	σ_{xz}	σ_{yz}
NA	448	1.35	-6.80	-84.78	0.189	19.4	419.4	272.0	-3.4	3.7	-310.6

^aAngular velocity vectors specify plate motion in ITRF2005, with positive angular rotation rates corresponding to counterclockwise rotation about the pole. N is the number of GPS site velocities used to determine the best-fitting angular velocity vector. Here χ^2_ν is the weighted least-squares fit divided by the number of velocity components ($2*N$) minus 3, the number of parameters adjusted to fit the data. All covariances are propagated linearly from the GPS site velocity uncertainties and have been rescaled so that the final χ^2_ν equals 1.0. The rotation rate ω has units of degrees per million years. Angular velocity covariances are Cartesian and have units of 10^{-12} radians² per Ma². Abbreviation: NA, North American plate.

noise in the daily station locations [Marquez-Azua and DeMets, 2003], resulting in typical daily scatter of 1–3 mm in the horizontal station coordinates relative to running 10-day average locations. Linear regression of the three geocentric station coordinates, including corrections for any offsets due to antenna hardware changes or relocations, is used to estimate station velocities.

[13] An empirically derived error model that approximates the white and flicker noise in each station time series and incorporates 1 mm per \sqrt{a} of assumed random monument walk [Mao et al., 1999] is used to estimate the velocity uncertainties. Our estimates of the amplitudes of the white and flicker noise are similar to those reported by Williams et al. [2004] for the SOPAC global solution and give rise to station velocity uncertainties of ± 0.5 – 0.9 mm a⁻¹ for most of the RGNA stations spanning the 5.6-year-long period from early 2003 to mid-2008 (Table 1). Langbein [2008] uses best geodetic noise models derived from GPS time series for stations in southern California and Nevada to estimate that the uncertainties for 5-year-long GPS time series should range from 0.1 to 0.6 mm a⁻¹ for a range of different monumentation types, modestly smaller than but comparable to the uncertainties we estimate for the RGNA time series. Our analysis focuses on deformation signals faster than ~ 1 mm a⁻¹ and is thus robust with respect to these small differences in the estimated velocity uncertainties. Uncertainties at the other 448 North American plate stations, whose time series span 3.0 to 15.6 years, range from ± 0.3 to 2 mm a⁻¹.

4.2. North American Plate Reference Frame

[14] The North American plate constitutes the natural geological reference frame for describing and interpreting the motions of RGNA stations in mainland Mexico. The motion of the plate relative

to ITRF2005 is strongly constrained by the many continuous GPS stations from undeforming areas of the plate interior. We derived a best-fitting angular velocity vector from the velocities of 448 North American plate GPS stations (Figure 2), most ($\sim 75\%$) of which are located in the central and eastern United States. The angular velocity vector that best fits these velocities (Table 2) is determined using fitting functions described by Ward [1990]. For reasons described by Argus [1996] and Blewitt [2003], Earth's center of mass is the appropriate geo-origin for tectonic studies such as this. We thus corrected all of the RGNA and North American plate station velocities for the estimated motion of the ITRF2005 geocenter relative to Earth's center of mass before inverting those velocities to determine their best-fitting angular velocity vector. On the basis of results reported by Argus [2007], we apply respective corrections of 0.3, 0.0, and 1.2 mm a⁻¹ to the X, Y, and Z Cartesian station velocity components.

[15] The residual components of the 448 North American plate GPS station velocities (Figure 2) have a weighted root-mean-square misfit of 0.63 mm a⁻¹, close to the lower end of the ± 0.3 to 2 mm a⁻¹ range of the estimated velocity uncertainties. Reduced chi-square for the best-fitting angular velocity vector is 1.35, indicating that the average velocity misfit is $\sim 15\%$ (i.e., $\sqrt{1.35}$) larger than its assigned uncertainty. The WRMS misfits are therefore only ~ 0.1 mm a⁻¹ larger than the average estimated uncertainties of ± 0.5 – 0.6 mm a⁻¹. This difference is too small to affect our analysis, which focuses on deformation that is faster than ~ 1 mm a⁻¹.

[16] Some of the stations whose velocities are used to estimate North American plate motion lie west of the Rockies and Rio Grande rift (Figure 2), where slow deformation may occur. We thus inverted the velocities of only those stations that lie east of the Rockies and Rio Grande rift in order to examine whether this significantly alters our estimate of North American plate motion in Mex-

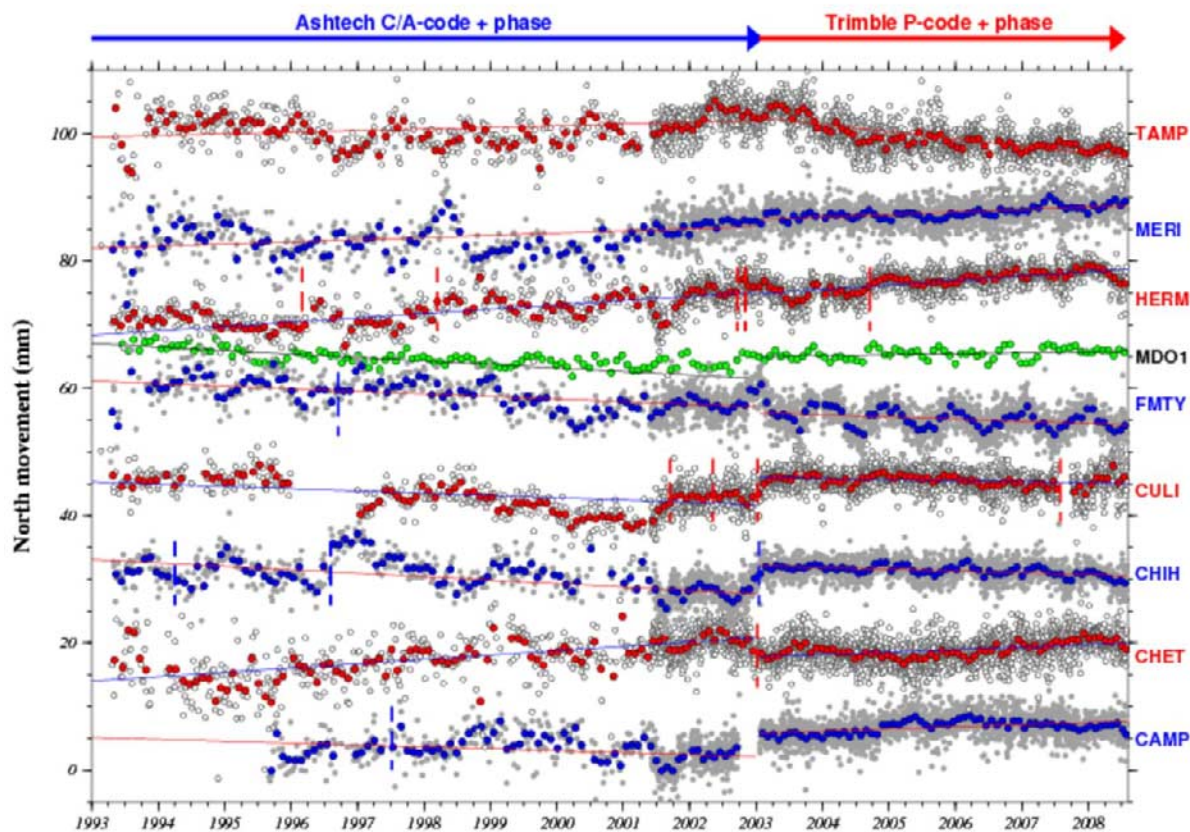


Figure 3. Time series of north components of GPS station coordinates for RGNA stations north of the Mexican Volcanic belt and in the Yucatan peninsula and station MDO1 in southern Texas. Site motions are specified relative to the North American plate (Table 2). Vertical dashed lines show times of offsets that have been estimated and removed from the station time series. Gray and open circles show daily station positions. Monthly average station positions are shown by green, red, and blue circles. Solid lines best fit the station coordinates from 1993.0 to 2001.5, the interval spanned by the codeless Ashtech data, and 2003.0 to 2008.6.

ico. The alternative best-fitting angular velocity vector predicts station motions in Mexico that differ by no more than 0.02 mm a^{-1} from the motions that are predicted by the angular velocity vector given in Table 2, too small to affect any aspect of the analysis below.

[17] All of the station velocities and coordinate time series described below were transformed to a North American plate frame of reference by subtracting the plate motion predicted at each site by the best-fitting angular velocity vector (Table 2). Uncertainties in the best-fitting angular velocity vector were propagated rigorously into all station velocity uncertainties quoted in the text and shown in the figures.

5. Results

[18] Our results are presented in two stages. We first use the station coordinate time series for nine

RGNA sites with linear motion (Figures 3–5) to test for significant differences in the station velocities before and after the GPS receiver changeover that occurred in 2003. We then use the new RGNA site velocities to evaluate the fits of two geologically plausible models for the present motion and deformation of Mexico. The analysis concludes with descriptions of the motions of stations OAXA and TOLU (Figure 5), which exhibit the elastic effects of steady interseismic locking and transient slip along the Cocos plate subduction interface, and of stations COLI and INEG, whose motions are strongly influenced by the coseismic and postseismic effects of subduction thrust earthquakes off the coast of western Mexico on 9 October 1995 and 22 January 2003 (Figure 8).

5.1. RGNA Stations With Linear Motions

[19] Figures 3–5 show the coordinate time series for all nine RGNA stations with linear motions

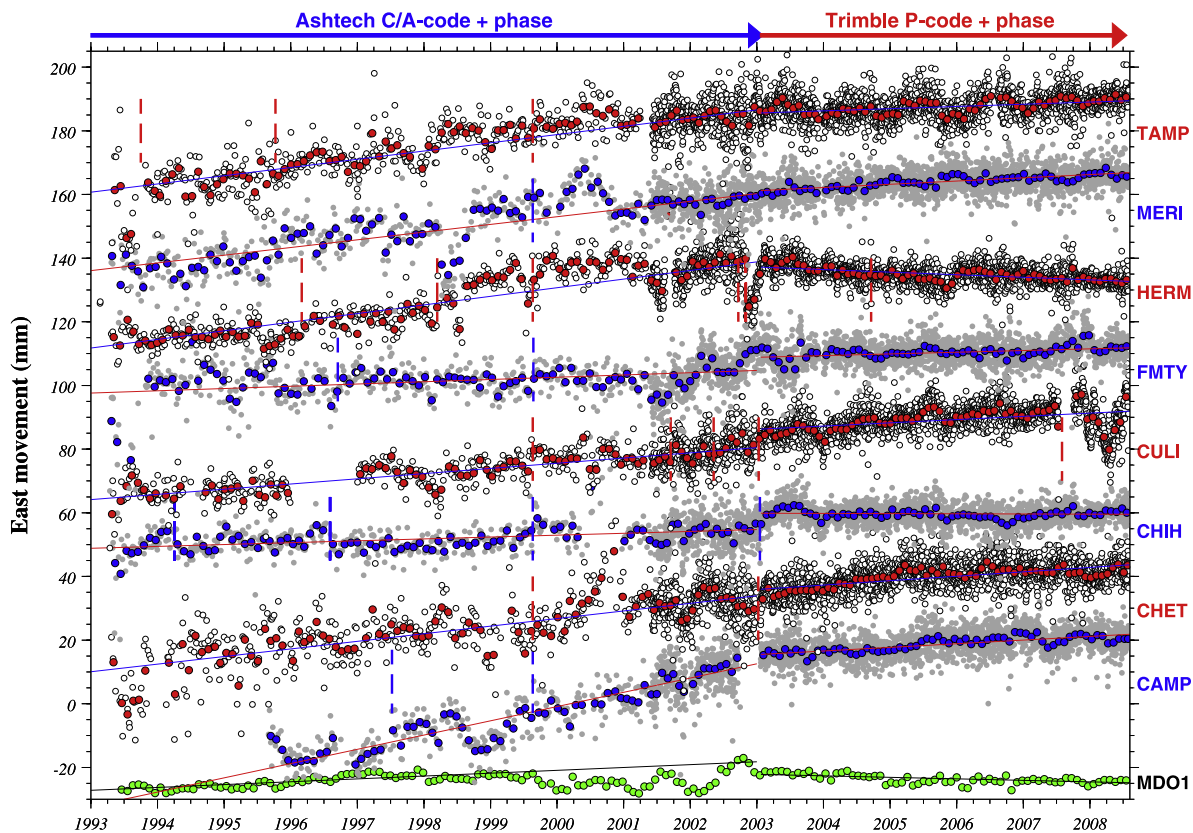


Figure 4. Time series of east component of GPS station coordinates for RGNA stations north of the Mexican Volcanic belt and in the Yucatan peninsula, and station MDO1 in southern Texas. See caption to Figure 3 for additional information.

from mainland Mexico and one station (MDO1) in southern Texas at which continuous P-code carrier phase GPS measurements have been made since 1993. The steady motions at the RGNA sites provide a strong basis for comparing the site motions during the period from 1993 to 2003, when data at all nine stations were collected by Ashtech C/A-code receivers, to the motions since 2003.0, during which P-code Trimble receivers have operated at all nine sites.

[20] We first test for significant changes in the north components of the station motions before and after 2003 by deriving separate best-fitting lines for the daily station coordinates from 1993 to 2003 and for 2003 to the present (mid-2008). The slopes that best fit the RGNA station latitudes during these two time periods differ on average by 0.7 mm a^{-1} , with differences at the individual sites of 0.2 mm a^{-1} to 1.3 mm a^{-1} (Figure 3). None of the changes in slope at the nine RGNA stations are significant at the 95% confidence level.

[21] At site MD01 in Texas, where dual-frequency P-code GPS data has been collected continuously

since 1993, the slopes that best fit the daily station coordinates for times before and after 2003 differ by 0.8 mm a^{-1} . The difference in slope at MDO1 before and after 2003 is thus comparable to that for the RGNA sites, where the differences average 0.7 mm a^{-1} .

[22] We conclude that the north (latitudinal) components of the RGNA station motions are well determined for the entire period that the sites have operated. Transient deformation episodes that were recorded before 2003 at RGNA sites OAXA and TOLU (described below) were dominated by north–south station movements and by implication were also reliably recorded.

[23] The east components of motion at the nine RGNA stations are less consistent (Figure 4). The differences between the best-fitting rates for the two time periods range from 0.2 to 3.4 mm a^{-1} and average 1.6 mm a^{-1} , more than twice the average slope difference for the station latitudes. At seven of the nine RGNA sites, the eastward site motion before 2003.0 was faster by 1 – 3.5 mm a^{-1} than

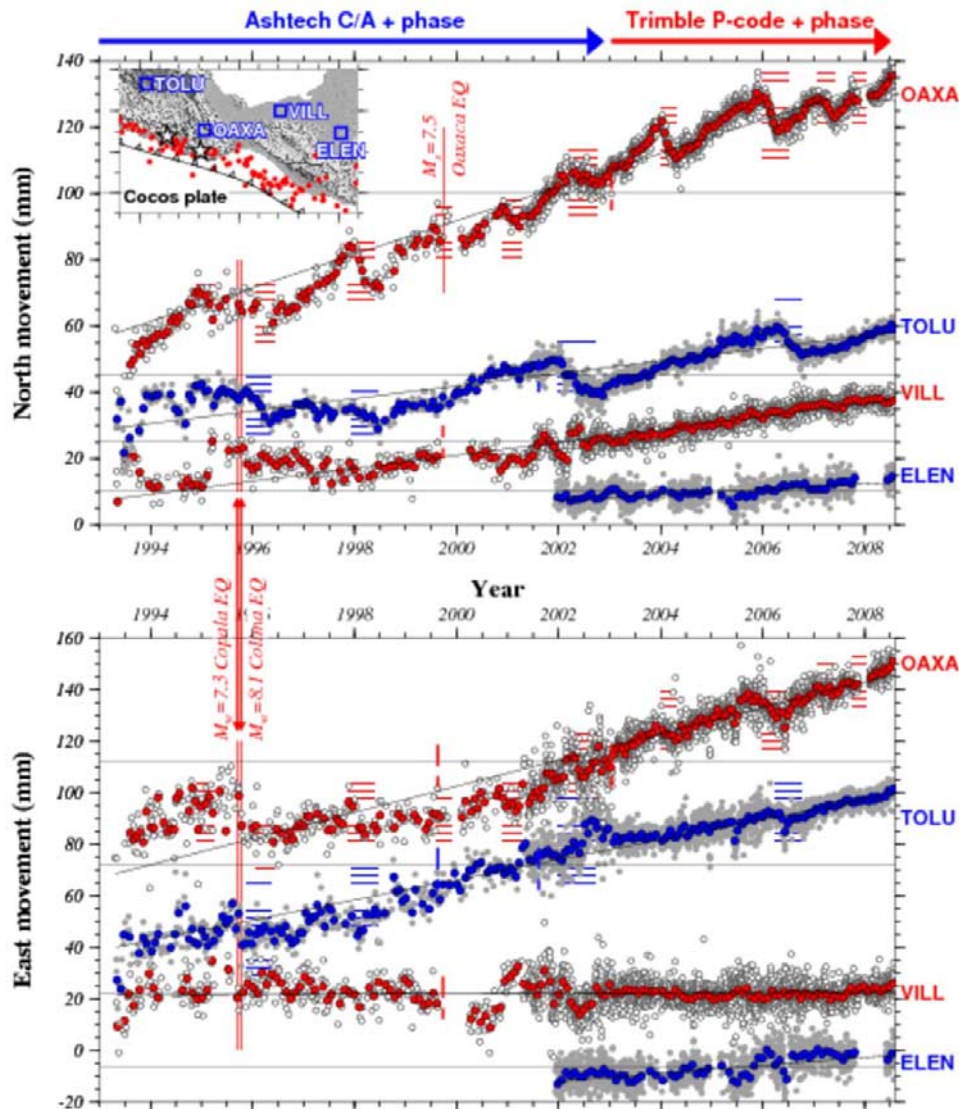


Figure 5. (top) North and (bottom) east components of GPS station coordinates from 1993 to 2008 for RGNA stations in southern Mexico and station ELEN in Guatemala. Patterned areas specify periods of southward station motion that coincide with transient slip along the subduction interface. See caption to Figure 3 for additional information. Inset shows topography, GPS station locations, and epicenters (red circles) of 1963–2008 earthquakes with magnitudes greater than 5.5 and depths above 40 km from the U.S. Geological Survey National Earthquake Information Center files. Black stars in inset show locations of the $M_w = 7.3$ 14 September 1995 Copala and $M_s = 7.5$ 30 September 1999 Oaxaca earthquakes.

after 2003.0 (Figure 4), and at five sites, the change in slope is statistically significant.

[24] The evidence thus indicates that there was a systematic, significant change in the apparent east component of the station motions in early 2003, coinciding with the change in GPS equipment at most of the stations. All four stations in and near the Yucatan peninsula that were reported by MD2003 as having anomalously rapid eastward motion slowed down significantly after 2003 (com-

pare blue and red velocities at sites CAMP, CHET, MERI, and VILL in Figure 6).

[25] We thus conclude that east components of the RGNA station motions for times when the Ashtech LM-XII3 codeless receivers were operating, primarily before 2003.0, are unreliable. We suspect but cannot show that the receiver firmware or hardware corrupted the raw data. The coordinate time series for station MDO1 (Figures 4 and 5) and other P-code stations in the southern United States

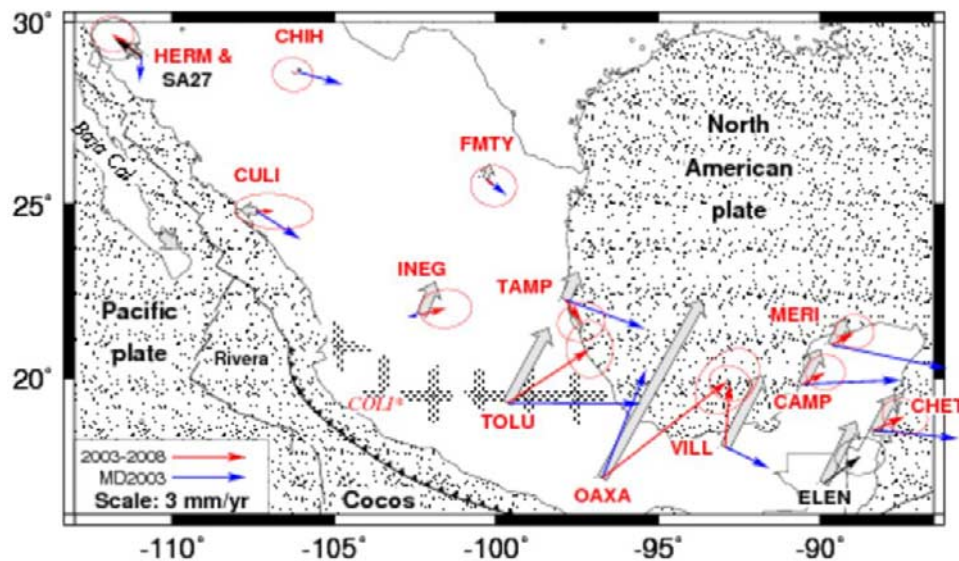


Figure 6. RGNA station velocities relative to the North American plate for sites on mainland Mexico. Red arrows show velocities determined solely from 2003 to 2008.6 P-code carrier phase GPS data and blue arrows show velocities determined by *Marquez-Azua and DeMets* [2003] from Ashtech codeless data from 1993 to 2001.5. Gray arrows indicate velocities predicted by an elastic half-space model with a fully coupled Mexican subduction interface and faults in the Gulf of California, as described in the text. The velocity for station COLI is severely impacted by postseismic effects of the $M_w = 8.0$ 9 October 1995 earthquake and $M_w = 7.5$ 22 January 2003 earthquake and is not depicted. Uncertainty ellipses are 2-D, 1- σ .

that have operated since at least the mid-1990s (not shown) do not exhibit significant changes in their north or east components of motion before and after 2003, further reinforcing the above conclusion.

5.2. Velocity Field Analysis

[26] We next undertake statistical comparisons of three realizations of the RGNA station motions to velocity fields that are predicted by two models for the present motion and deformation of Mexico. In the first model, we assume that all of mainland Mexico moves with an undefining North American plate. In the second model, we assume that the elastic effects of frictional coupling across the Mexican subduction zone and strike-slip faults in the Gulf of California are superimposed on the plate motion. Further details about both models are given below.

[27] The three RGNA velocity fields used for this comparison consist of the MD2003 velocities for 1993 to 2001.5, velocities from 1993 to 2003.0, which span the entire period of Ashtech LM-XII3 codeless measurements, and velocities from 2003.0 to August of 2008 (Table 1), which span the period of Trimble P-code, carrier phase measurements at the RGNA sites. Each velocity field includes 12 of

the 13 RGNA stations, consisting of all nine linearly moving sites (Figures 3 and 4) and the velocities for INEG, OAXA, and TOLU, whose long-term motions are contaminated to varying degrees by transient deformation related to the Mexican subduction zone (described in section 5.3). We excluded site COLI from this part of the analysis because its motion is too severely disrupted by the coseismic and postseismic effects of the 9 October 1995 $M_w = 8.0$ and 22 January 2003 earthquakes (described in section 5.3.2) to recover any useful information about either the long-term motion or interseismic elastic shortening at this site.

[28] We use weighted root-mean-square (WRMS) misfits to evaluate the fits of both models to the three velocity fields described above. We gauge the acceptability of the fit of each model to the observed velocities by comparing it to the 0.63 mm a^{-1} WRMS misfit of the angular velocity that best fits the 448 North American plate station velocities. The WRMS misfit for these 448 stations should approximate the underlying velocity dispersion for GPS stations located in a plate interior and therefore should be an approximate limit on how well we might expect any model to fit the RGNA station velocities. Although more complex physical models for the present motion and deformation of Mexico could

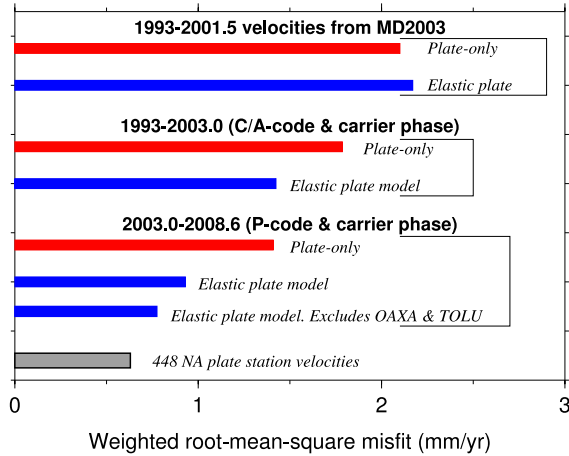


Figure 7. Weighted root-mean-square misfits of the North American plate angular velocity vector (plate-only) and elastically modified plate models to RGNA velocity fields for stations on mainland Mexico. Red and blue bars indicate fits of plate-only and elastic plate models, respectively. The gray bar shows the RMS misfit to the 448 station velocities used to determine the North American plate angular velocity vector. Fits for three realizations of the RGNA velocities are shown: the 1993–2001.5 velocities from *Marquez-Azua and DeMets* [2003], velocities determined from 1993–2003 Ashtech data described in the text, and velocities determined from 2003.0–2008.6 P-code and carrier phase GPS data. Unless otherwise noted, the fits are determined for 12 of the 13 RGNA stations on the mainland and exclude only station COLI due to postseismic effects from the 9 October 1995 and 22 January 2003 earthquakes.

be postulated and tested, we demonstrate below that the RGNA station velocities are fit at the level of their uncertainties by one of the two simple models that we tested.

5.2.1. Plate-Only Model

[29] The simplest of the two models we examined assumes that the motion of mainland Mexico is well described by the angular velocity vector that best fits the 448 North American station velocities (Table 2). The residual motions of the RGNA stations relative to the North American plate for the 1993–2001.5 MD2003 site velocities (blue arrows in Figure 6) clearly reveal the east-directed velocity bias described by MD2003. In contrast, the residual motions for the new 2003–2008.6 velocities show no obvious systematic bias (red arrows in Figure 6). The WRMS misfit to the 1993–2001.5 MD2003 station velocities is 2.1 mm a⁻¹ (Figure 7), more than three times larger than for the 448 North American plate station

velocities. We measured the statistical significance of the difference between these two fits using a F ratio test comparison of the ratio of the values of reduced chi-squared for the two models. The fits differ at a high confidence level ($p = 8 \times 10^{-7}$). The MD2003 RGNA station velocities therefore differ significantly from the velocities predicted by the North American plate angular velocity vector.

[30] The WRMS misfit of the plate-only model to the station velocities averaged from 1993 through early 2003 is 1.8 mm a⁻¹ (Figure 7), only marginally better than for the 1993–2001.5 MD2003 velocity field (Figure 7). This misfit also differs at high confidence level from the misfit to the 448 North American plate station velocities.

[31] The WRMS misfit of the plate-only model to the 2003.0–2008.6 RGNA velocities is 1.4 mm a⁻¹ (Figure 7), smaller than for the other two velocity fields. The velocities of all of the stations north of the volcanic belt except HERM are well fit by the plate-only model (red arrows in Figure 6). The motions at sites in central Mexico, southern Mexico, and the Yucatan peninsula however differ systematically from the plate-only model predictions. The WRMS misfit is still more than twice the magnitude of the WRMS misfit for the 448 North American plate station velocities and differs at high confidence level ($p = 1 \times 10^{-7}$). We conclude that none of the RGNA velocity fields are well fit by a plate-only model.

5.2.2. Velocity Field Analysis: Elastically Modified Plate Model

[32] The second model we tested superimposes the interseismic elastic effects of frictional coupling across faults in the Gulf of California and the Mexican subduction zone on North American plate motion. The elastic response at each RGNA station due to assumed locking of both sets of faults is determined using homogeneous elastic half-space modeling. Each of the strike-slip fault segments in the Gulf of California is assumed to be locked from the surface to a maximum depth of 10 km, representing an approximate conservative depth limit for the seismogenic zone in the Gulf of California [Goff *et al.*, 1987]. The interseismic elastic response is determined assuming that a 48 mm a⁻¹ slip deficit accumulates along each strike-slip fault in the gulf, consistent with the average slip rate in the Gulf over the past 0.78 Ma [DeMets, 1995].

[33] The Mexican subduction zone is approximated with 360 nodes whose locations in the elastic half



space mimic the geography of the subduction zone (node locations are shown in Figure 1) and define a planar fault that dips 15° beneath the continent and extends downdip to a depth of 25 km, the approximate lower limit of seismogenic slip for the Mexican subduction interface [Suarez and Sanchez, 1996; Hutton *et al.*, 2001; Yoshioka *et al.*, 2004; Correa-Mora *et al.*, 2008]. The elastic responses at the RGNA sites are determined by imposing trench-normal back slip at each node that is equal in magnitude to the convergence rate calculated from either the Rivera-North America [DeMets and Wilson, 1997], Cocos-North America [DeMets, 2001], or Cocos-Caribbean [DeMets, 2001] angular velocity vector, depending on the node location. The model thus implicitly assumes that the subduction interface is fully and homogeneously coupled by friction at depths above 25 km. Although this model clearly oversimplifies the interseismic behavior and geometry of the Mexican subduction interface, the RGNA stations are too widely spaced and in most cases too far from the trench to merit any additional model complexity. As described below, this surprisingly simple model approximates the northeast-directed elastic shortening of mainland Mexico well enough to fit most of the RGNA station velocities to better than 1 mm a^{-1} .

[34] The predicted elastic responses at the RGNA stations (shown by the gray arrows in Figure 6) range from less than 0.1 mm a^{-1} at sites in northern Mexico to 8.4 mm a^{-1} at station OAXA in southern Mexico. Changes of $\pm 5^\circ$ in the assumed 15° dip of the subduction interface alter the rates that are predicted by our elastic half-space model by $\sim 20\%$, representing one source of uncertainty in our elastic model predictions.

[35] The WRMS misfit of the elastically modified model to the MD2003 velocity field is nearly the same as for the plate-only model (Figure 7) and still differs at high confidence level ($p = 9 \times 10^{-7}$) from the WRMS misfit to the 448 North American station velocities. Similarly, the WRMS misfit to the 1993–2003 station velocities (1.4 mm a^{-1}) also differs from that for the 448 North America station velocities at high confidence level ($p = 4 \times 10^{-5}$). Neither of the two RGNA velocity fields that are determined from the Ashtech data are consistent within acceptable limits with the predictions of the plate-only or elastically modified models.

[36] The WRMS misfit of the elastically modified model to the 2003–2008.6 P-code velocity field is 0.93 mm a^{-1} 35% smaller than the WRMS misfit of the plate-only model (Figure 7). More than half

of the variance (56%) between the measured and predicted station velocities is contributed by the poor fits at stations OAXA and TOLU (Figure 6). The poor fits are not surprising given that the motions of both stations are influenced by transient slip events (Figure 5), which are ignored in our simplified elastic model. In addition, the approximations that we use to construct our elastic model influence the motions predicted by that model at OAXA and TOLU by as much as $1\text{--}3 \text{ mm a}^{-1}$. The misfits thus could be reduced if we changed one or more of our modeling assumptions.

[37] If we exclude the velocities at OAXA and TOLU, the WRMS misfit of the elastically modified model to the remaining 10 RGNA station velocities is only 0.77 mm a^{-1} , close to the 0.63 mm a^{-1} WRMS misfit for the 448 North American plate stations. The values of reduced chi-square associated with these two fits do not differ significantly ($p = 0.42$). The velocities of the stations far from the subduction zone are thus consistent with the hypothesis that mainland Mexico moves with the North American plate after the elastic effects of locked plate boundary faults are accounted for.

[38] Although the poor fits to the velocities at sites OAXA and TOLU prevent us from concluding that areas south of the Mexican volcanic belt also move with the North American plate, Correa-Mora *et al.* [2008] find that the directions of 30 GPS stations in Oaxaca, south of the volcanic belt, differ by less than 1° from the Cocos-North America plate convergence direction after correcting the station time series for the influence of transient slip episodes. Their results thus indicate that southern Mexico moves with the North America plate, in accord with structural evidence for insignificant Quaternary displacement across faults in the Mexican volcanic belt [Ferrari and Rosas-Elguera, 2000; Suter *et al.*, 2001; Langridge *et al.*, 2000].

5.3. RGNA Stations With Nonlinear Motions

[39] All four of the RGNA stations that are located within several hundred kilometers of the Mexican subduction zone exhibit nonlinear motions (Figures 5 and Figure 8) that represent superpositions of subduction-related processes and North American plate motion. Their coordinate time series provide useful new information about the timing, style, and spatial extent of deformation in southern Mexico and are described below. Modeling of these and other non-RGNA time series is underway to relate all four time series to earthquake cycle effects

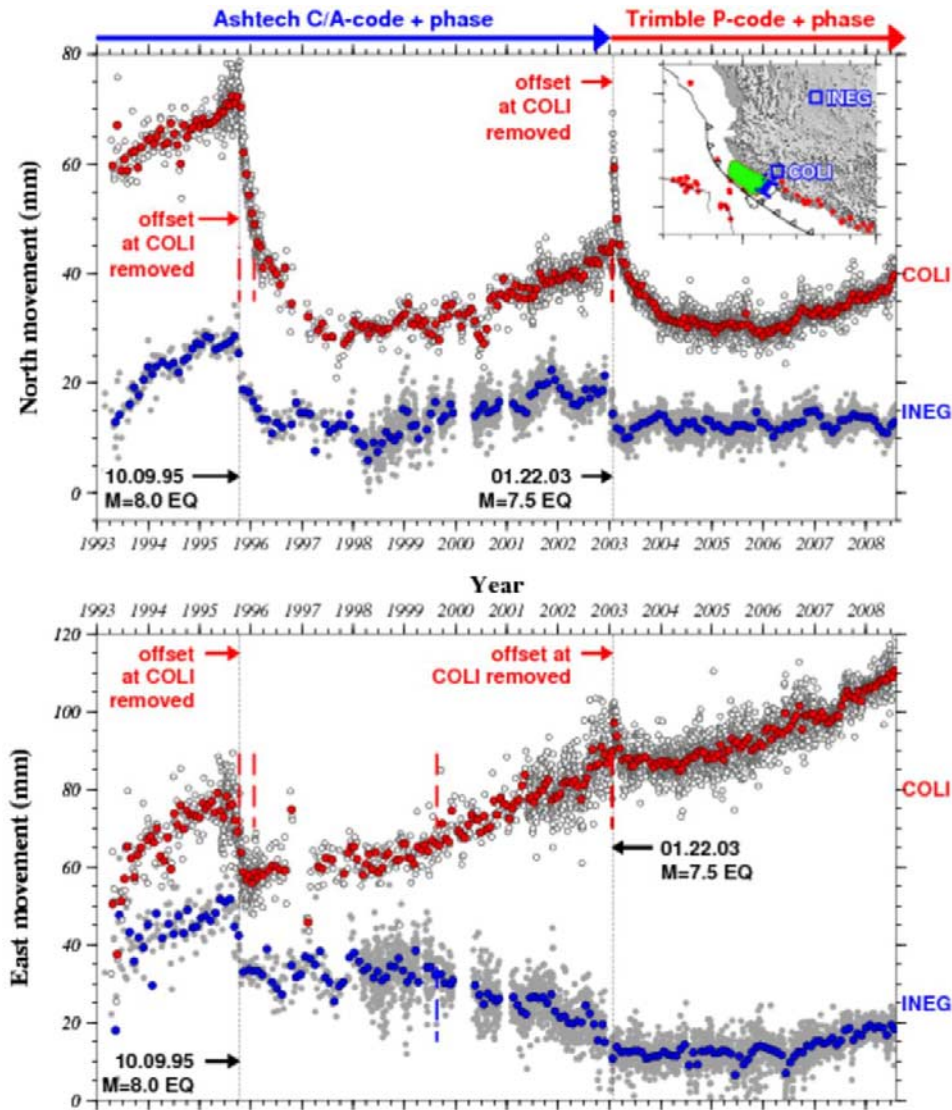


Figure 8. Modified (top) north and (bottom) east components of GPS station coordinates from 1993 to 2008 for RGNA stations COLI and INEG in western Mexico. Arbitrary offsets at COLI for the 9 October 1995, $M_w = 8.0$ Colima-Jalisco and 22 January 2003, $M_w = 7.5$ Tecoman earthquakes have been removed from the time series in order to enhance the postseismic and interseismic phases of the time series. Inset shows topography, GPS station locations, and epicenters (red circles) of 1963–2008 earthquakes with magnitudes greater than 5.5 and depths above 40 km from the U.S. Geological Survey National Earthquake Information Center files. See caption for Figure 3 for additional information about the symbols and dashed lines. Green and blue shaded regions in inset show extent of the 1995 and 2003 earthquakes. See caption to Figure 3 for additional information.

associated with the Cocos and Rivera plate subduction interfaces.

5.3.1. Effects of Transient Slip Events in Southern Mexico

[40] Stations OAXA and TOLU lie onshore from the Oaxaca and Guerrero segments of the Mexican subduction zone (Figure 5), where continuous measurements at these and other GPS stations reveal evidence for occasional transient slip events

along parts of the subduction interface downdip from the seismically active areas of the subduction interface [Lowry *et al.*, 2001; Kostoglodov *et al.*, 2003; Franco *et al.*, 2005; Brudzinski *et al.*, 2007; Larson *et al.*, 2007; Correa-Mora *et al.*, submitted manuscript, 2009]. Although the net motions of both stations since 1993 have been northeast with respect to the plate interior, both stations have alternated between periods of northeast-directed motion that last from one to several years and



periods of opposite-sense, trenchward motion that last from 2 to 6 months.

[41] Ten periods of transient slip were recorded at OAXA between 1993 and mid-2008 (Figure 5), all dominated by south-directed motion, but including lesser west-directed motion. The magnitudes of the SSW-directed transient offsets range from 5 mm to 15 mm, of which the largest were in early 1998, early 2004, and early 2006, and smaller episodes were in early 1995, early 1996, late 1999, late 2000, mid-2002, and early 2007. Modeling of the transient slip events in 2004, 2006, and 2007 indicates that all three occurred beneath eastern Oaxaca downdip from the seismogenic zone [Brudzinski *et al.*, 2007; Correa-Mora *et al.*, 2008; Correa-Mora *et al.*, submitted manuscript, 2009]. Modeling of the earlier transient slip events has not been undertaken due to the sparse continuous GPS station coverage prior to 2004.

[42] Two moderate- to large-magnitude earthquakes occurred along the Guerrero and Oaxaca segments of the Mexican subduction zone between 1993 and mid-2008: the 14 September 1995 $M_w = 7.3$ Copala earthquake, a thrust-faulting event along the Guerrero trench segment ~ 200 km west of OAXA (see Figure 5 inset), and the 30 September 1999 $M_s = 7.5$ Oaxaca earthquake, a normal faulting event within the subducting Cocos plate beneath central Oaxaca. During the Copala earthquake, an offset of ~ 10 mm toward the rupture zone west of Oaxaca was recorded at station OAXA (shown in Figure 5, bottom). During the 1999 Oaxaca intraslab earthquake, no coseismic offset was recorded at OAXA. Interestingly, the 1999 earthquake occurred during the transient slip event recorded at OAXA in late 1999, suggesting the possibility that one may have triggered the other. The OAXA station positions for this period are, however, too noisy to determine whether the earthquake preceded the initiation of transient slip or vice versa.

[43] Fewer transient slip events have been recorded at station TOLU, which is located in the Mexican volcanic belt inland from the Guerrero segment of the subduction zone (Figure 5). Three or possibly four transient slip events have been recorded since 1993, each dominated by 7–15 mm of southward motion toward the Guerrero segment of the Mexican subduction zone. The earliest transient slip episode began in late 1995 and is clearly shown by the reliably recorded N–S component of motion at TOLU. From campaign GPS measurements in 1995, 1996, and 1998 along the coast of Guerrero,

Larson *et al.* [2004] hypothesize that transient slip occurred beneath Guerrero in late 1995. The RGNA measurements confirm this.

[44] Transient slip events that were recorded at TOLU in early 1998, 2001–2002, and 2006 (Figure 5) coincide with transient slip events beneath Guerrero that are described and modeled by Lowry *et al.* [2001], Kostoglodov *et al.* [2003], and Larson *et al.* [2007]. Readers are referred to those studies for additional information.

5.3.2. COLI and INEG: Effects of the 1995 and 2003 Western Mexico Earthquakes

[45] The 9 October 1995 $M_w = 8.0$ Colima-Jalisco earthquake and 22 January 2003 $M_w = 7.5$ Tecoman earthquake (Figure 8) ruptured the Rivera/Cocos plate subduction interfaces off the coast of western Mexico. Both caused measurable coseismic and postseismic movements at stations COLI and INEG (Figure 8), which are located 80 km and 400 km inland from the coast, respectively. During the 1995 earthquake, COLI was offset by 132 ± 5 mm toward $S66^\circ W$ [Marquez-Azua *et al.*, 2002], toward the seismologically and geodetically constrained region of maximum coseismic slip [Melbourne *et al.*, 1997; Mendoza and Hartzell, 1999; Hutton *et al.*, 2001]. Additional trenchward motion occurred during the following 18 months (Figure 8), consisting largely of ~ 50 mm of southward movement at rates that decayed with time. By early 1998, slow northeastward movement had resumed, similar to the site motion before the earthquake.

[46] Finite element modeling of the COLI coordinate time series for 1993 to mid-2001 suggests that three distinct processes contributed to the station motion during this period: (1) steady, northeast-directed elastic shortening due to frictional locking of shallow seismogenic parts of the subduction interface, (2) decaying postseismic fault afterslip in response to time-dependent changes in the coefficient of friction after the 1995 earthquake, (3) decaying viscoelastic relaxation of the elevated stresses in the lower crust and upper mantle after the earthquake [Marquez-Azua *et al.*, 2002].

[47] During the 2003 earthquake, COLI was offset 127 ± 5 mm toward $S34^\circ W$, consistent with the coseismic offsets that were measured at other stations in this region [Schmitt *et al.*, 2007]. The station continued moving to the SSW at increasingly slower rates for 18–24 months after the earthquake (Figure 8) and resumed moving slowly



to the northeast by early 2006. The similarity of the postseismic movements after the 1995 and 2003 earthquakes suggests that fault afterslip, viscoelastic rebound, and frictional relocking of shallow seismogenic areas of the subduction interface controlled the surface deformation at COLI in both cases, providing a solid basis for better understanding the physical processes that dictate short-term deformation in this region.

[48] Although groundwater withdrawal caused station INEG to subside more than 1.4 m between early 1993 and August of 2008 (not shown), the rapid station subsidence does not appear to have corrupted its horizontal motion, which mimics many features of the COLI time series since 1993 (Figure 8). We attribute the differences in the motions of INEG and COLI to their different distances from the subduction zone, which gives rise to less interseismic elastic shortening at INEG than at COLI, as well as relatively less viscoelastic rebound at INEG after the 1995 and 2003 earthquakes. We are presently modeling these and other data from the region to better understand the relative contributions of viscoelastic rebound, fault afterslip, and interseismic locking to earthquake cycle deformation in this region.

6. Discussion and Conclusions

[49] The elastically modified plate model described above is remarkably effective at predicting the newly estimated RGNA velocity field (Figure 6). In particular, our updated velocities for the four RGNA stations in and near the Yucatan peninsula (CAMP, CHET, MERI, and VILL) agree within their uncertainties with the northeast-directed station motions that are predicted by our simple elastic model (Figure 6). The puzzling eastward bias reported by MD2003 in the velocities for these four stations was thus an artifact of the non-P-code Ashtech data that were used to estimate the MD2003 velocities. Similar eastward biases in the velocities estimated by MD2003 at other RGNA stations (Figure 6) were thus also artifacts of the Ashtech data and are largely gone from the updated velocity field. Overall, the WRMS difference between the model predictions and updated station velocities is only 0.8 mm a^{-1} , comparable to the misfit for the 448 station velocities that were inverted to determine the North American plate angular velocity vector.

[50] At station HERM east of the Gulf of California (Figure 6), our elastic model predicts motion of

0.8 mm a^{-1} toward $\text{N}55^\circ\text{W}$, the same within uncertainties as the measured velocity of $1.4 \pm 0.6 \text{ mm a}^{-1}$ toward $\text{N}53^\circ\text{W} \pm 21^\circ$. Further supporting this result, GPS site SA27, which has operated continuously since mid-2003 at a location only 1.5 km from HERM, also moves $1.2 \pm 0.6 \text{ mm a}^{-1}$ toward $\text{N}55^\circ\text{W} \pm 29^\circ$ (Figure 6), nearly the same as HERM and in even better agreement with the elastically predicted motion. Incorporating the elastic effects of locked strike-slip faults in the Gulf of California is thus necessary for fitting these station velocities.

[51] Our simple elastic model successfully predicts the northeastward motions of RGNA stations INEG, OAXA, and TOLU in central and southern Mexico (Figure 6) but fits those velocities more poorly than is the case at the other RGNA sites. The poorer fits are due in part to the effects of transient slip episodes at both sites, which influence their estimated motions. Oversimplifications in our elastic half-space model also surely contribute to the misfits. We did not attempt to improve the fits by adjusting any of our elastic modeling assumptions or parameters, mainly because the RGNA stations are too widely spaced and too far from the trench to merit such an exercise. We instead refer readers who seek more information about the spatial and temporal characteristics of strain accumulation and release along the Cocos plate subduction interface to detailed modeling studies of GPS measurements at numerous near-coastal stations in Guerrero and Oaxaca [e.g., Yoshioka *et al.*, 2004; Franco *et al.*, 2005; Correa-Mora *et al.*, 2008].

[52] Although our new velocity field agrees much better with the predictions of our simple elastic model than does the MD2003 velocity field, small differences between the newly measured velocities and the predicted velocities still remain. In particular, the velocities of six of the seven RGNA stations in the volcanic belt, southern Mexico, and the Yucatan peninsula are rotated clockwise from the predicted motions by varying amounts (Figure 6), as is the velocity of station ELEN in northern Guatemala. Random errors in the estimated station velocities are unlikely to cause this systematic difference. Although the velocity bias is consistent with slow eastward motion ($\sim 1 \text{ mm a}^{-1}$ or less) of southern Mexico and northern Guatemala relative to the North American plate, a more conservative interpretation is that the time series for all of these stations are still too short (5 to 6 years) to effectively average out any time-correlated variations in the station coordinates that remain coherent over



periods of several years or longer. Additional years of observations will help to reduce the effect of time-correlated noise. To determine whether GPS system noise might be responsible for some or all of the small remaining eastward velocity bias, we also plan to reprocess the RGNA data using the next generation of satellite orbits and geodetic reference frame products that should soon be available from the International GNSS Service.

Acknowledgments

[53] We thank INEGI for generously providing daily data from the RGNA network, without which this work would not be possible. We thank Luca Ferrari and an anonymous reviewer for their helpful suggestions. This research was funded by National Science Foundation grant EAR-0510553 and by the University of Guadalajara, which contributed funds for research exchange visits.

References

- Altamimi, Z., X. Collilieux, J. Legrand, B. Garayt, and C. Boucher (2007), ITRF2005: A new release of the International Terrestrial Reference based on time series of station positions and Earth Orientation parameters, *J. Geophys. Res.*, *112*, B09401, doi:10.1029/2007JB004949.
- Argus, D. F. (1996), Postglacial uplift and subsidence of Earth's surface using VLBI geodesy: On establishing vertical reference, *Geophys. Res. Lett.*, *23*, 973–976.
- Argus, D. F. (2007), Defining the translational velocity of the reference frame of Earth, *Geophys. J. Int.*, *169*, 830–838, doi:10.1111/j.1365-246X.2007.03344.x.
- Bennett, R. A., J. L. Davis, and B. P. Wernicke (1999), Present-day pattern of Cordilleran deformation in the western United States, *Geology*, *27*, 371–374.
- Blewitt, G. (2003), Self-consistency in reference frames, geocenter definition, and surface loading of the solid Earth, *J. Geophys. Res.*, *108*(B2), 2103, doi:10.1029/2002JB002082.
- Brudzinski, M., E. Cabral-Cano, F. Correa-Mora, C. DeMets, and B. Marquez-Azua (2007), Slow slip transients along the Oaxaca subduction segment from 1993 to 2007, *Geophys. J. Int.*, *171*, 523–538, doi:10.1111/j.1365-246X.2007.03542.x.
- Calais, E., J. Y. Han, C. DeMets, and J. M. Nocquet (2006), Deformation of the North American plate interior from a decade of continuous GPS data, *J. Geophys. Res.*, *111*, B06402, doi:10.1029/2005JB004253.
- Correa-Mora, F., C. DeMets, E. Cabral-Cano, B. Marquez-Azua, and O. Diaz-Molina (2008), Interplate coupling and transient slip along the subduction interface beneath Oaxaca, Mexico, *Geophys. J. Int.*, *175*, 269–290, doi:10.1111/j.1365-246X.2008.03910.x.
- DeMets, C. (1995), A reappraisal of seafloor spreading lineations in the Gulf of California: Implications for the transfer of Baja California to the Pacific plate and estimates of Pacific-North America motion, *Geophys. Res. Lett.*, *22*, 3545–3548.
- DeMets, C. (2001), A new estimate for present-day Cocos-Caribbean plate motion: Implications for slip along the Central American volcanic arc, *Geophys. Res. Lett.*, *28*, 4043–4046.
- DeMets, C., and D. S. Wilson (1997), Relative motions of the Pacific, Rivera, North American, and Cocos plates since 0.78 Ma, *J. Geophys. Res.*, *102*, 2789–2806.
- Dixon, T., F. Farina, C. DeMets, F. Suarez Vidal, J. Fletcher, B. Marquez-Azua, M. Miller, O. Sanchez, and P. Umhoefer (2000), New kinematic models for Pacific-North America motion from 3 Ma to present, II: Tectonic implications for Baja and Alta California, *Geophys. Res. Lett.*, *27*, 3961–3964.
- Ferrari, L., and J. Rosas-Elguera (2000), Late Miocene to Quaternary extension at the northern boundary of the Jalisco block, western Mexico: The Tepic-Zacoalco rift revisited, in *Cenozoic Tectonics and Volcanism of Mexico*, edited by H. Delgado-Granados, G. Aguirre-Diaz, and J. Stock, *Geol. Soc. Am. Spec. Pap.*, *334*, 41–64.
- Franco, S. I., V. Kostoglodov, K. M. Larson, V. C. Manea, M. Manea, and J. A. Santiago (2005), Propagation of the 2001–2002 silent earthquake and interplate coupling in the Oaxaca subduction zone, Mexico, *Earth Planets Space*, *57*, 973–985.
- Goff, J. A., E. A. Bergman, and S. C. Solomon (1987), Earthquake source mechanisms and transform fault tectonics in the Gulf of California, *J. Geophys. Res.*, *92*, 10,485–10,510.
- Guzman-Speziale, M., and J. J. Meneses-Rocha (2000), The North America-Caribbean plate boundary west of the Motagua-Polochic fault system: a fault jog in southeastern Mexico, *J. S. Am. Earth Sci.*, *13*, 459–468.
- Guzman-Speziale, M., W. D. Pennington, and T. Matumoto (1989), The triple junction of the North America, Cocos, and Caribbean plates: Seismicity and tectonics, *Tectonophysics*, *8*, 981–997.
- Heflin, M., et al. (1992), Global geodesy using GPS without fiducial sites, *Geophys. Res. Lett.*, *19*, 131–134.
- Hutton, W., C. DeMets, O. Sanchez, G. Suarez, and J. Stock (2001), Slip kinematics and dynamics during and after the 1995 October 9 $M_w = 8.0$ Colima-Jalisco earthquake, Mexico, from GPS geodetic constraints, *Geophys. J. Inter.*, *146*, 637–658.
- Kostoglodov, V., S. K. Singh, J. A. Santiago, S. I. Franco, K. M. Larson, A. R. Lowry, and R. Bilham (2003), A large silent earthquake in the Guerrero seismic gap, Mexico, *Geophys. Res. Lett.*, *30*(15), 1807, doi:10.1029/2003GL017219.
- Langbein, J. (2008), Noise in GPS displacement measurements from southern California and southern Nevada, *J. Geophys. Res.*, *113*, B05405, doi:10.1029/2007JB005247.
- Langridge, R. M., R. J. Weldon, II, J. C. Moya, and G. Suarez (2000), Paleoseismology of the 1912 Acambay earthquake and the Acambay-Tixmadeje fault, Trans-Mexican Volcanic Belt, *J. Geophys. Res.*, *105*, 3019–3037.
- Larson, K. M., A. R. Lowry, V. Kostoglodov, W. Hutton, O. Sanchez, K. Hudnut, and G. Suarez (2004), Crustal deformation measurements in Guerrero, Mexico, *J. Geophys. Res.*, *109*, B04409, doi:10.1029/2003JB002843.
- Larson, K. M., V. Kostoglodov, S. Miyazaki, and J. A. S. Santiago (2007), The 2006 aseismic slow slip event in Guerrero, Mexico: New results from GPS, *Geophys. Res. Lett.*, *34*, L13309, doi:10.1029/2007GL029912.
- Lowry, A., K. Larson, V. Kostoglodov, and R. Bilham (2001), Transient fault slip in Guerrero, southern Mexico, *Geophys. Res. Lett.*, *28*, 3753–3756.
- Mao, A., C. G. A. Harrison, and T. H. Dixon (1999), Noise in GPS coordinate time series, *J. Geophys. Res.*, *104*, 2797–2816.
- Marquez-Azua, B., and C. DeMets (2003), Crustal velocity field of Mexico from continuous GPS measurements, 1993 to June, 2001: Implications for the neotectonics of Mexico, *J. Geophys. Res.*, *108*(B9), 2450, doi:10.1029/2002JB002241.
- Marquez-Azua, B., C. DeMets, and T. Masterlark (2002), Strong interseismic coupling, fault afterslip, and viscoelastic flow before and after the Oct. 9, 1995 Colima-Jalisco earthquake:



- Continuous GPS measurements from Colima, Mexico, *Geophys. Res. Lett.*, *29*(8), 1281, doi:10.1029/2002GL014702.
- Marquez-Azua, B., E. Cabral-Cano, F. Correa-Mora, and C. DeMets (2004), A model for Mexican neotectonics based on nationwide GPS measurements, 1993–2001, *Geof. Int.*, *43*, 319–330.
- Melbourne, T., I. Carmichael, C. DeMets, K. Hudnut, O. Sanchez, J. Stock, G. Suarez, and F. Webb (1997), The geodetic signature of the M8.0 October 9, 1995, Jalisco subduction earthquake, *Geophys. Res. Lett.*, *24*, 715–718.
- Mendoza, C., and S. Hartzell (1999), Fault-slip distribution of the 1995 Colima-Jalisco, Mexico, earthquake, *Bull. Seismol. Soc. Am.*, *89*, 1338–1344.
- Michaud, F., et al. (2004), Motion partitioning between the Pacific plate, Baja California, and the North America plate: The Tosco-Abreojos fault revisited, *Geophys. Res. Lett.*, *31*, L08604, doi:10.1029/2004GL019665.
- Plattner, C., R. Malservisi, T. H. Dixon, P. LaFemina, G. Sella, J. Fletcher, and F. Vidal-Suarez (2007), New constraints on relative motion between the Pacific plate and Baja California microplate (Mexico) from GPS measurements, *Geophys. J. Int.*, *170*, 1373–1380, doi:10.1111/j.1365-246X.2007.03494.x.
- Schmitt, S. V., C. DeMets, J. Stock, O. Sanchez, B. Marquez-Azua, and G. Reyes (2007), A geodetic study of the 2003 January 22 Tecoman, Colima, Mexico earthquake, *Geophys. J. Int.*, *169*, 389–406, doi:10.1111/j.1365-246X.2006.03322.x.
- Sella, G. F., S. Stein, T. H. Dixon, M. Craymer, S. James, S. Mazzotti, and R. K. Dokka (2007), Observation of glacial isostatic adjustment in “stable” North America with GPS, *Geophys. Res. Lett.*, *34*, L02306, doi:10.1029/2006GL027081.
- Suarez, G., and O. Sanchez (1996), Shallow depth of seismogenic coupling in southern Mexico: Implications for the maximum size of earthquakes in the subduction zone, *Phys. Earth Planet. Int.*, *93*, 53–61.
- Suter, M., M. López Martínez, O. Quintero Legorreta, and M. Carrillo Martínez (2001), Quaternary intra-arc extension in the central Trans-Mexican volcanic belt, *Geol. Soc. Am. Bull.*, *113*, 693–703.
- Ward, S. N. (1990), Pacific-North America plate motions: New results from very long baseline interferometry, *J. Geophys. Res.*, *95*, 21,965–21,981.
- Williams, S. D. P., Y. Bock, P. Fang, P. Jamason, R. M. Nikolaidis, L. Prawirodirdjo, M. Miller, and D. J. Johnson (2004), Error analysis of continuous GPS time series, *J. Geophys. Res.*, *109*, B03412, doi:10.1029/2003JB002741.
- Yoshioka, S., T. Mikumo, V. Kostoglodov, K. M. Larson, A. R. Lowry, and S. K. Singh (2004), Interplate coupling and a recent aseismic slow slip event in the Guerrero seismic gap of the Mexican subduction zone, as deduced from GPS data inversion using a Bayesian information criterion, *Phys. Earth Planet. Inter.*, *146*, 513–530.
- Zumberge, J. F., M. B. Heflin, D. C. Jefferson, M. M. Watkins, and F. H. Webb (1997), Precise point positioning for the efficient and robust analysis of GPS data from large networks, *J. Geophys. Res.*, *102*, 5005–5017.